

Propagating uncertainty from catchment experiments to estimates of streamflow reduction by invasive alien plants in southwestern South Africa

Glenn R. Moncrieff^{1,2}, Jasper A. Slingsby^{1,3}, and David C. Le Maitre^{4,5}

¹Fynbos Node, South African Environmental Observation Network (SAEON), Cape Town, Western Cape, South Africa

²Centre for Statistics in Ecology, the Environment and Conservation, Department of Statistical Sciences, University of Cape Town, Cape Town, Western Cape, South Africa ³Centre for Statistics in Ecology, the Environment and Conservation, Department of Biological Sciences, University of Cape Town, Cape Town, Western Cape, South Africa ⁴CSIR Natural Resources and the Environment, Stellenbosch, South Africa

⁵Centre for Invasion Biology, Department of Botany and Zoology, Stellenbosch University, South Africa

Running title: Uncertainty in streamflow reduction

Abstract: Long-term catchment experiments from South Africa have demonstrated that afforestation of grasslands and shrublands significantly reduces surface-water runoff. These results have guided the country's forestry policy and the implementation of a national Invasive Alien Plant (IAP) control programme for the past few decades. Unfortunately, woody IAP densities continue to increase, compounding existing threats to water security from population growth and climatic change. Decision makers need defensible estimates of the impacts of afforestation or invasions on runoff to weigh up alternative land use options, or guide investment of limited resources into ecosystem restoration through IAP clearing versus engineering-based water-augmentation schemes. Existing attempts to extrapolate the impacts observed in catchment afforestation experiments to broad-scale IAP impacts give no indication of uncertainty. Globally, the uncertainty inherent in the results from paired-catchment experiments is seldom propagated into subsequent analyses making use of these data. We present a fully reproducible Bayesian model that propagates uncertainty from input data to final estimates of changes in streamflow when extrapolating from catchment experiments to broader landscapes. We apply our model to South Africa's catchment experiment data, estimating streamflow losses to plantations and analogous plant invasions in the catchments of southwestern South Africa, including uncertainty. We estimate that regional streamflow is reduced by 304 million m³ or 4.14% annually as a result of IAPs, with an upper estimate of 408

This article has been accepted for publication and undergone full peer review but has not been through the copyediting, typesetting, pagination and proofreading process which may lead to differences between this version and the [Version of Record](#). Please cite this article as doi: [10.1002/hyp.14161](https://doi.org/10.1002/hyp.14161)

million m³ (5.54%) and a lower estimate of 267 million m³ (3.63%). Our model quantifies uncertainty associated with all parameters and their contribution to overall uncertainty, helping guide future research needs. Acknowledging and quantifying inherent uncertainty enables more defensible decisions regarding water resource management.

Keywords: South Africa | Invasive alien plants | Uncertainty partitioning | Runoff reduction | Paired catchment | Beta regression | Afforestation | Catchment experiment

Corresponding author: glenn@saeon.ac.za

1. Introduction

South Africa is a water stressed country with a mean annual precipitation of around 500 mm. Large parts of the country are subject to high or extremely high overall water risk (Hofste et al., 2019). Temporal variability in water stress is also large, with severe droughts regularly impacting the environment, society and economy (Schreiner et al., 2018). Most recently, the period 2015-2017 saw a multiyear drought in southwestern South Africa, with the lowest recorded rainfall of the last century (Bischoff-Mattson et al., 2020; Sousa et al., 2018). The drought affected the entire winter rainfall region of South Africa, with the City of Cape Town and its 3.7 million residents threatened with 'Day Zero' - the day domestic water supplies would be cut off. It is estimated that the 2015-2017 drought cost the region's economy around ZAR 5.9 billion (approx. USD 400 million) and resulted in the loss of 30 000 jobs (Pienaar & Boonzaier, 2018). The magnitude and impact of droughts in the region are expected to increase with population growth and climate change. A drought of the magnitude experienced between 2015-2017 is already 3 times more likely due to existing climate change (Otto et al., 2018). Climatic change is expected to decrease runoff for the western Cape province between 2% and 17% by 2050 (Kalognomou et al., 2013; Sousa et al., 2018; Steynor et al., 2009).

Similar droughts in the 1920s reinforced growing concerns about the impact of replacing native grasslands and shrublands with plantation forestry on water resources. These events led to the establishment of a series of catchment-scale afforestation experiments across the country, beginning in the late 1930s (Bennett & Kruger, 2013). Results from these experiments showed that forestry species drastically reduce streamflow relative to indigenous shrublands and grasslands (Scott & Smith, 1997). Concern was subsequently raised about impacts on water resources due to afforestation, predominantly through plantation forestry and the associated spread of woody invasive alien plant (IAP) species from these plantations. While large differences exist among species, abundant species such as Wattles (*Acacia spp.*), Pines (*Pinus spp.*) and Eucalypts (*Eucalyptus spp.*) use up to 20% more water than native species through higher evapotranspiration and interception rates (Le Maitre et al., 2015). These differences have been used to guide water use licensing for plantation forestry, and form the primary motivation behind the creation of a national IAP clearing programme (Van Wilgen et al., 1998). While plantation forestry may be justified on the basis of economic benefits, the outcomes of spreading IAPs are almost entirely negative, reducing streamflow (Le Maitre et al., 2015), impacting on biodiversity (Slingsby et al., 2017), and increasing fire risk (Kraaij et al., 2018). Despite attempts to control the spread of IAPs they continue to increase in range, diversity and

abundance (van Wilgen et al., 2020). The most recent national assessment estimated that invasions in 2008 occupied the equivalent of 15000 km² of the land area of South Africa (Kotze et al., 2010). The Western Cape province was the worst affected region with the equivalent of 2300 km² of dense invasions. Attempts to quantify the impacts of IAPs on surface water availability at the national and regional scale have built upon data from the catchment experiments (Cullis et al., 2007; Le Maitre et al., 2019, 2016; Versfeld et al., 1998). The most recent national analysis (Le Maitre et al., 2016) combined data on the distribution and abundance of 26 IAP species (Kotze et al., 2010) and updated information on the water-use of IAPs (Le Maitre et al., 2015) with the streamflow reductions measured in the catchment experiments (Scott & Smith, 1997). The Le Maitre et al. (2016) analysis estimated that as of 2008 on average 1 443.56 million m³ or 2.88% of South Africa's annual surface water runoff was lost to IAPs. The Western Cape alone was losing 355.42 million m³ per year or 5.1% of runoff. A more focused assessment of subcatchments that feed the major dams supplying water to the City of Cape Town and surrounds - the Western Cape Water Supply System (WCWSS) - estimated that the system was losing 38 million m³ of the 98% assured yield per year as of the year 2000, increasing to 130 million m³ per year by 2045 if the invasions were not managed (Le Maitre et al., 2019). Given the city's target water use of 0.45 million m³ per day at the height of the 2015-2017 drought, this volume of water translates into about 3 and 9 months of water supply respectively.

All attempts at calculating runoff loss to IAPs in South Africa have failed to quantify the degree of uncertainty around estimates or parameter values. This failure is due to a number of factors including the computational requirements for calculating probabilistic forecasts on spatial models, a lack of data on uncertainty in input parameters, and the paucity of gauged catchments with which to evaluate models (Kapangaziwiri et al., 2012; Yanai et al., 2018). Without any quantification of how much confidence they can have in an estimate of current water losses, decision makers will not have adequate information with which to weigh risks and evaluate the benefits of clearing IAPs against other options for alleviating water stress (Reichert & Borsuk, 2005). Furthermore, quantifying the sources of uncertainty can help researchers focus their data collection and/or model development efforts to improve model performance (Harmon et al., 2015). Of particular concern are the curves used to describe the data on afforestation effects on streamflow obtained from the catchment experiments. Scott & Smith (1997) fitted a range of models to these data, and reported the best fitting curves. These curves have been used in numerous subsequent assessments of forestry water use and the broader

scale impact of IAPS on streamflow (Le Maitre et al., 2019; Scott et al., 1998; Versfeld et al., 1998). While they provide a good overall fit to the experimental catchment data, they only provide point estimates of the expected streamflow reductions.

Models that report uncertainty in their parameter estimates would allow the full range of possible outcomes to be evaluated, and the uncertainty from these models may then be propagated to estimates of streamflow reduction. Incorporating the uncertainty in the data and parameters used to drive simulations is common in hydrological models (Beven & Binley, 1992; Kavetski et al., 2006; Vrugt & Sadegh, 2013). Typically models are run many times with the full range of prior possible parameter values and forcing data, and outputs compared to in-situ data from gauged catchments. These simulations can in turn be used to evaluate model fit, and create improved posterior estimates of parameters. However, when in-situ data is not available, models must extrapolate from other catchments. Streamflow reduction curves have been used in multiple studies as the basis for this extrapolation (Versfeld et al., 1998, Le Maitre et al., 2019). But few paired catchment studies report directly on the uncertainty in experimental results (Brown et al., 2005; but see Scott & Smith, 2000). As a result this observational error is not carried through to models attempting to model hydrological changes in other catchments through the extrapolation of data from paired catchment experiments.

In order to provide decision-makers with the best available information to manage water resources, and guide future research into the impacts of afforestation and IAPs on water resources, we revisit the streamflow reduction curves fitted to the South African experimental catchment data (Scott & Smith, 1997). We fit models to these data and fully characterize the uncertainty in model predictions. Using these models, we then propagate this uncertainty to projections of water resources impact of land cover change in ungauged basins using the model of Le Maitre et al. (2016) for estimating impacts of IAPs on streamflow in southwestern South Africa. Specifically, we set out to:

1. Select and fit an appropriate model for estimating streamflow changes from experimental catchment data within a Bayesian framework.
2. Based on these curves, update and include uncertainty in the estimates of the volume and percent of streamflow lost to IAPs from the catchments of southwestern South Africa.
3. Calculate the relative contribution of various sources of uncertainty to overall uncertainty in streamflow losses to guide efforts to improve future estimates, such as through model development, new experiments and data collection.

4. Ensure that estimates can quickly and easily be recalculated as and when updated data become available or model improvements are made by adopting an open science approach, using only open-source software and sharing all data and code to provide a fully repeatable workflow.

2. Methods

2.1 Model overview

We limit our model to the Cape Floristic Region (CFR), a phytogeographic region of 108677 km² encompassing most of the Western Cape province and South Africa's winter and all-year rainfall regions (Figure S1, Bergh et al., 2014), to take advantage of existing climate interpolations that provide uncertainty estimates (Wilson & Silander Jr., 2014). The approach taken by Le Maitre et al. (2016) distills decades of experience and expert knowledge, condensing the existing literature on water use by IAPs into a tractable model for the countries of South Africa, Lesotho and Swaziland (Le Maitre et al., 2020). The impact of IAPs on water resources can be assessed by applying catchment-level hydrological models to simulate discharge within a region of interest. Streamflow reductions can be investigated by changing vegetation parameterisation (e.g Gush et al. 2002; Qiao et al. 2015). This approach is preferable when the study area is limited to a few quaternary catchments due to data and computational requirements. These models require detailed parameterisations and observations that are not available for the numerous species and ungauged catchments included in this study. The Le Maitre et al. (2016) approach is built around a conceptual model which proposes that water-use is limited by certain plant traits - assuming a climatically stable environment and rainfall as the only water source (Calder, 1985, 2005). Shifts in the traits of the dominant species lead to changes in the relationship between rainfall and runoff (Bosch & Hewlett, 1982; Zhang et al., 2001). The streamflow reduction curves fitted to the data from the South African catchment experiments show how species with different trait archetypes change the rainfall-runoff relationship in a particular environment. If we assign IAP species to one of these archetypes we can assume similar impacts on runoff (Le Maitre et al., 2015). The high-level logical flow of our model is outlined in Figure 1 and described briefly below:

The study area is subdivided into 306 catchments and modeled on a 250m x 250m pixel scale, corresponding to the resolution of the most recent data on the distribution of IAP species in the region (Kotze et al. 2010). A nested hierarchy of catchments is used as planning units in South

Africa, ranging from primary drainage basin, through to secondary and tertiary, with the smallest operational unit being the quaternary catchment. The 306 catchments used here are defined at the quaternary level, and average 650 km² in size.

First, the proportional reduction in mean annual runoff due to all IAPs within each pixel is calculated using the fitted streamflow reduction curves based on the age and density of each species. Next, the potential mean annual runoff in each pixel is calculated by converting mean annual rainfall to naturalized runoff (expected runoff in the absence of anthropogenic influence) using established rainfall-runoff relationships. After removing the proportion of runoff lost to IAPs, and adjusting for additional water use in riparian zones and areas with access to groundwater, the remaining pixel-level runoff is summed for each quaternary catchment. Full details and rationale are given in Le Maitre et al. (2016).

Below under each subheading we briefly describe how each of the above mentioned components are parameterised, elaborating on additions and modifications to the original model and the representation and propagation of uncertainty. The contribution of each of these components to overall uncertainty is also quantified separately.

2.2 Streamflow reduction curves

Scott and Smith fitted asymptotic curves to data collected in South African's multidecadal catchment experiments. Scott et al. (2000) describe these data in detail and the overall results of the catchment experiments. Selected catchments were afforested with commonly planted forestry species (*Pinus spp.* and *Eucalyptus spp.*) in a variety of habitats and paired with nearby, comparable catchments with natural vegetation. Afforestation began after a calibration period in which a sufficiently reliable relationship between runoff in the paired catchments had been established. This relationship was used to predict naturalized runoff in the afforested catchments based on the observed runoff in the catchment with natural vegetation. Observed and predicted runoff were then compared over time and the absolute and percentage runoff reduction occurring as a result of afforestation calculated for each year that streamflow was monitored. Nonlinear curves were then fit to predict the percentage runoff reduction observed as a function of plantation age. Scott & Smith (1997) distinguished between catchments afforested with either *Pinus spp.* and *Eucalyptus spp.* and between catchments with either optimal or sub-optimal growing conditions for the planted tree species, resulting in 4 separate curves for total flow reduction. Numerous previous studies (e.g. Le Maitre et al. 2019; Scott et

al. 1998; Versfeld et al. 1998) have used these streamflow reduction curves to estimate runoff loss following afforestation or alien plant invasion in South Africa. We refit curves similar to those presented in Scott & Smith (1997) using Beta regression. We use data from 10 catchments distributed across South Africa described in detail by Scott et al. (2000). As plantations reach maturity and canopy closure, streamflow reductions asymptote, and sometimes even decline. Similar to Scott & Smith (1997), we do not include a term to account for this decline, and exclude data for mature plantations where this effect is pronounced from our analysis. This exclusion is defensible, because the natural vegetation in our region of interest typically burns every 10-30 years, the IAPs are flammable, and stands are unlikely to reach an age where streamflow reductions begin to decline. Beta regression is the appropriate class of model when the response variable is a proportion (Ferrari & Cribari-Neto, 2004). Beta regression uses the beta distribution as the likelihood for the data,

$$f(y_i|a,b) = \frac{y_i^{(a-1)}(1-y_i)^{(b-1)}}{B(a,b)}$$

where $B(\cdot)$ is the beta function and y_i is the percentage reduction in streamflow observed in each year. The shape parameters for the distribution, a and b , enter into the model according to the following transformations

$$a = \mu \cdot \phi b = (1 - \mu) \cdot \phi$$

The expected value of y is μ . For a given value of μ , larger ϕ implies smaller variance, and hence it is known as the precision parameter. μ is modelled as a function of predictor variables

$$\mu = \text{logit}^{-1}(\mathbf{X}\boldsymbol{\beta})$$

where \mathbf{X} is a $N \times (K + 1)$ dimensional matrix of K predictors and an intercept term for N observations, and β is a $K + 1$ dimensional vector of parameters associated with each predictor. As done by Scott & Smith (1997), three predictor variables are used in the beta regression: stand age, growing condition (optimal or sub-optimal), and species (Pine or Eucalypt). We fit multiple models testing interactions of age, condition and species, and select the best fitting model based on the LOOIC (leave-one-out cross-validation information criterion) (Vehtari et al., 2017). Location parameters (β) are given uninformative normal priors and precision parameters (ϕ) uninformative Cauchy priors. Model fitting is conducted using Markov chain Monte Carlo (MCMC) with the No-U-Turn-Sampler (NUTS) implemented in Stan (Carpenter et al., 2017). Three separate MCMC chains are fitted each with 2000 iterations. Parameter sampling begins after a warmup of 1000 iterations. Chains were monitored to ensure satisfactory convergence and mixing. Parameter samples from the best fitting model were then used to estimate streamflow losses to IAPs, propagating the uncertainty in streamflow reduction curves from the data of Scott & Scott (2000) to our estimates. This probabilistic approach differs from Le Maitre et al. (2016), where the deterministic curves from Scott et al. (2000) were used.

In order to calculate streamflow lost as a result of each species for which data is available, species must be assigned to a particular curve. Thus for each species we must assess whether the slope fitted to Pines or Eucalypts is more appropriate. Similarly we must determine whether a species occurs in optimal or sub-optimal conditions. While for some species this assignment is trivial (eg. Wattles (*Acacia spp.*) affect streamflow in a similar manner to Eucalypts) for others it is not clear. Le Maitre et al. (2016) assigned species in a binary manner to curves based on expert knowledge and previous research on water use of prominent IAPs (Le Maitre et al., 2015). We use the same approach, though we assign species to curves probabilistically (e.g. species can be assigned with an 50% chance to the Eucalypt curve or 50% chance to the Pine curve if the appropriate choice is unclear). The full table of species and curves to which they are assigned is available in Table S1.

2.3 Potential runoff

Spatially interpolated precipitation data is generally accessed in the form of a single map providing the mean annual or monthly value at a given pixel (e.g. Fick & Hijmans 2017; Schulze 1997). The use of a single pixel mean often obscures the high uncertainty associated with rainfall interpolated in mountainous areas, in which the spatial and temporal density of precipitation observations is low (Fick & Hijmans, 2017). This issue is particularly important in

the CFR, where most runoff is generated by precipitation occurring in poorly sampled, remote mountain catchment areas (Nel et al., 2017). Wilson & Silander Jr (2014) used a Bayesian framework to interpolate 20 years of daily meteorological observations into climate surfaces for the CFR. These climate surfaces provide a full characterization of uncertainty associated with each pixel. From these climate surfaces we calculate the mean and standard deviation of mean annual precipitation at 1-km resolution over the CFR. Naturalized runoff (runoff that would have occurred under natural land cover without dams, diversions or abstraction) generated at each pixel is calculated using these precipitation surfaces and converted to runoff using rainfall-runoff curves specifically calibrated for groups of catchments with similar hydrological behaviour using the Pitman hydrological model (Midgley et al., 1994). Total catchment-level runoff is calculated by summing over all pixels and compared to the expected naturalized runoff (Bailey & Pitman, 2015). This ratio is used to rescale pixel-level runoff estimates, ensuring that biases in the simple rainfall-runoff curves do not result in biased estimates of naturalized runoff at the catchment level. This exact process to calculate runoff at the pixel-scale was used in Le Maitre et al. (2016), but rather than use probabilistic precipitation data, deterministic values were obtained from Schultze et al. (1997). Unfortunately, neither the rainfall-runoff curves from Scott & Smith (1997) nor the naturalized runoff estimates from Bailey & Pitman (2015) are associated with measures of uncertainty. Therefore our estimate of uncertainty in naturalized runoff is based entirely on the spatial uncertainty in mean annual precipitation.

2.4 Additional water availability

At many locations in the landscape additional water is available to plants (Le Maitre et al., 2015), including riparian areas and where groundwater is within the rooting depth. In these locations, and where evaporation from vegetation is driven mainly by the available energy, the total evaporation can exceed the annual rainfall. Spatially explicit estimates of where this additional water may be accessed by plants are not available, and hence Le Maitre et al. (2016) used a number of proxies to map these regions. The presence of azonal vegetation types and soil types conducive to the formation of deep root systems with access to aquifers were mapped by Le Maitre et al. (2016) and used to this end, based on data from Mucina & Rutherford (2006) and LTSS (2002). We used this same map, and added data from the recently compiled National Wetlands Map of South Africa version 5 (van Deventer et al., 2020). In mountainous regions of the CFR, groundwater interacts with vegetation and can produce surface flow. Groundwater dependent ecosystems are hotspots for rare and threatened

species, and are often heavily invaded by IAPs. Many of these groundwater seeps were not mapped in previous versions of the National Wetland Map as they can be very localized or only seasonally apparent. van Deventer et al. (2020) significantly improves the representation of these seeps, covering 453 748 ha nationally. We add these to the extent mapped by Le Maitre et al. (2016) as having access to groundwater. Additional water is also available to riparian vegetation. Le Maitre et al. (2016) used 1:500 000 maps of rivers and assumed the riparian zone to be 250m in width. This width estimate is a large overestimate and is intended to compensate for the underestimate of the total length of the rivers at 1:500 000 scale. We rather use 1:50 000 mapping and assume a riparian zone of 10m width. For ephemeral rivers, additional water in riparian zones is assumed to only be available to vegetation when they are flowing. The proportion of months with zero flow for each quaternary catchment were taken from Bailey & Pitman (2015) and applied to all ephemeral rivers within a catchment. Maps of ground and riparian water availability were created from the above-mentioned sources at 10m resolution. These were then aggregated to 250m resolution by calculating the proportion of each category in each 250m pixel. Flow reduction by IAPs in areas with groundwater access and in riparian zones are multiplied by a factor to represent the additional water use and higher impact of such invasions on streamflow loss. For all species this factor is sampled from a normal distribution with a mean of 1.2 and standard deviation of 0.2 when additional groundwater is accessible and a mean of 1.5 and standard deviation of 0.2 in riparian zones. The chosen mean value is taken from Le Maitre et al. (2016), where deterministic values were again used. These values are based on syntheses of research on IAP water use (Clulow et al., 2011; Le Maitre et al., 2016, 2015), and are gross approximations that ignore numerous factors influencing water use and availability, hence the need for probabilistic estimates.

2.5 Invasive Alien Plant density

The most recent assessment of the distribution and density of key IAP species across South Africa, Lesotho and Swaziland was completed by Kotze et al. (2010). The National Invasive Alien Plant Survey (NIAPS) reports on the number of hectares covered by 26 IAP species within landscape units - termed homogeneous mapping units (HMUs) - with similar physical and environmental conditions. Their models are trained using high resolution aerial photographs sampled at 74 000 locations across South Africa. The estimated density is reported for each IAP species in each HMU, with HMUs mapped at 250m resolution. For each species in each HMU, upper and lower estimates of density are provided. These estimates are based on the

variability observed across samples obtained within each HMU. We use these data to parameterise a mean and standard deviation of canopy cover percentage for each IAP in each HMU. Le Maitre et al. (2016) used only the mean canopy cover for each species within each HMU.

2.6 Vegetation age

Estimating streamflow reduction using the curves fitted to the data from South African catchment experiments requires an estimate of vegetation age analogous to the plantation age. The age effect represents the increasing water use of a fixed area of IAPs as they grow larger, accumulating greater leaf area and deeper roots. Le Maitre et al. (2016) assumed a uniform distribution around a mean vegetation age of between 10 and 20 years depending on the species under consideration. Much of the CFR is prone to stand-replacing natural wildfires, with a return time of 10-30 years. Most (though not all) IAPS are removed by these fires, and begin regrowth from seedbanks or resprouting. The expected fire return time is therefore a reasonable estimate to use for the age of an IAP stand. Wilson et al. (2010) used twenty years of fire occurrence data from across the CFR to fit a hierarchical Bayesian model of wildfire occurrence. With this model it is possible to estimate the expected fire return time as the age at which cumulative fire probabilities exceeds 50%. The analysis and results from Wilson et al. (2010) are limited to nature reserves in which fire data are routinely collected. To extend estimates of fire return time to the entire GCRF we used Bayesian spatial regression. Posterior samples of expected fire return time were used to fit a Bayesian spatial linear regression with mean annual precipitation and coefficient of variation of monthly precipitation estimated using the Wilson & Silander Jr (2014) climatic data as covariates. The model was fitted using MCMC implemented in the spBayes package (Finley et al., 2007) with priors for covariance parameters estimated by fitting a parametric model to the empirical variogram. One thousand maps of fire return time were sampled from the posterior predictive distribution and used in subsequent analyses. The fire return times estimated in regions where actual fire occurrence data is lacking are likely to be poorly constrained and hence highly variable. This simplification is however preferable to assuming a single vegetation age per species over the entire region as done by Le Maitre et al. (2016).

2.7 Simulations

All simulations are conducted in R (R Core Team, 2017). All data and code required to run our

model and reproduce our results are available at <https://github.com/GMoncrieff/streamflow-reduction>. We created probabilistic estimates of streamflow reduction by performing a Monte Carlo simulation, running our model 1000 times for each 250 x 250 meter pixel in the CFR (Figure 1).

1. For each model run we:
 - a. Assign each species to a specific streamflow reduction curve (optimal or sub-optimal, Eucalypt or Pine)
 - b. Sample a map of age over the CFR from the distribution of fire return time
 - c. Estimate proportional streamflow reduction for every IAP species using the assigned curve and age with a streamflow reduction curve sampled from posterior distribution of curves fitted to the South African catchment data.
 - d. Determine how much additional water is used by IAP in riparian zones and areas where groundwater is accessible
2. Within each run, for each catchment we
 - a. Sample the density of each IAP species
3. Within each catchment, for each pixel we
 - a. Estimate pixel-level naturalized runoff by sampling precipitation and converting to runoff
 - b. Correct for bias in naturalized runoff by summing naturalized runoff across all pixels within each quaternary catchment and rescaling to match estimates from Bailey & Pitman (2015)
 - c. Determine whether additional water in riparian zones or groundwater is accessible to IAPs
 - d. Calculate the runoff lost to IAPs by multiplying potential runoff from each pixel by the proportional streamflow reduction for every IAP species, and summing across all species.

These pixels-level estimates are then summed for each catchment in each model run yielding 1000 estimates of mean annual runoff loss for each catchment.

2.8 Uncertainty partitioning

Uncertainty partitioning is used to estimate the contribution of each input source of uncertainty

to the output uncertainty in streamflow reduction. The uncertainty attributed to each component is a combination of model sensitivity to an input and the uncertainty in the input itself (LeBauer et al., 2013). We do not perform a separate sensitivity analysis, as this analysis would require evaluating model prediction by varying input parameters by a specified value. The range over which to vary parameters should be determined by the reasonable range over which they might vary. Here we estimate this range by using the parameter values sampled from their distributions as defined in our model. Hence our uncertainty analysis is equivalent to a sensitivity analysis, with parameters variation determined using prior information. We can determine the relative contribution of a particular source of uncertainty to overall uncertainty in streamflow reduction by setting the uncertainty in all other inputs to zero. This simulation is performed for all uncertainty sources, namely: invasion density, curve assignment, age, streamflow reduction curves, additional water availability and precipitation. For each of these scenarios, we summarise the total uncertainty in estimated streamflow reduction at the catchment and pixel level using a robust estimate of dispersion - the median absolute deviation (MAD) - and the robust coefficient of variation (RCV_M) calculated as

$$RCV_M = 1.4826MAD/M$$

where MAD is the median absolute deviation and M median of streamflow reduction estimates across samples (Arachchige et al., 2019).

3. Results

The best fitting model to the streamflow reduction data from the South African catchments experiments included an age effect, a growing condition effect, a species effect, and an interaction term between age and growing condition (Table 1). The posterior predictive distributions for fitted curves are shown in Figure 2. Catchments afforested with Eucalypts showed greater reduction in streamflow than those afforested with Pines for a given age. Streamflow reductions for Pines growing in sub-optimal conditions were lower than those growing in optimal conditions, but for a given age the estimated reduction was highly variable with wide predictive intervals. No data was available for Eucalypts growing in sub-optimal conditions, and hence the effect of growing conditions fitted for Pines was applied. Our curves are similar to those fitted by Scott & Smith (1997), though they show a more gradual increase in

streamflow reduction with age. This difference results in higher estimates of streamflow reduction at young sites, and lower estimates at mature sites.

Using these curves to calculate streamflow losses across the CFR, we estimate that streamflow is reduced by a mean of 304 million m³ or 4.14% annually as a result of IAPs, with an upper estimate of 408 million m³(5.54%) and a lower estimate of 267 million m³(3.63%) using a 95% quantile interval. This estimate is slightly lower than the Le Maitre et al. (2016) estimates of 379 million m³ or 5.15% for the same 306 catchments. Overall there is good agreement between our estimates, (Figure 3, $R^2 = 0.89$, intercept = 0.10, slope = 0.73), though lower flow reductions are estimated for some high-flow catchments. Mean differences between our results and those from Le Maitre et al. (2016) are not due to nonlinear effects encountered when using parameters sampled probabilistically rather than mean values (Jensen, 1906). Mean catchment-level streamflow reduction estimates are near identical when sampling input data and parameters probabilistically vs. simply inputting mean values (Figure S2).

IAP impacts are concentrated spatially in a few regions of the CFR (Figure 4). From West to East these are: the sandy plains North of the City of Cape Town near Atlantis, the Cape Flats, the Hottentots-Holland and Franschoek-Villiersdorp mountain ranges, the Agulhas plain extending to Mossel Bay, the Tsitsikamma and Outeniqua coastal mountain ranges and Cape Recife near Port Elizabeth. The worst affected catchment, the Holsloot river in the Limietberg, is estimated to lose 32.9 million m³ per annum [24.7, 40.4] or 29.7% [22.3, 36.4] of total annual streamflow. The full distribution of posterior estimates of streamflow reduction for quaternary catchments surrounding the major dams that supply bulk water to the City of Cape Town is shown in Figure S3. The total reduction estimated for these catchments is 25.5 million m³ per annum [20.3,43.4] or 3.37% [2.68, 5.72] of total annual streamflow. Bimodal distributions evident in this figure are the results of uncertainty in assigning IAPs species to a particular streamflow reduction curve. Total uncertainty measures using *MAD* were highest in mountain catchments with high mean runoff and high streamflow losses, though many catchments with low runoff and low streamflow losses showed higher proportional uncertainty, measured using *RCV_M*(Figure 5). Overall, the largest contributing factor to uncertainty in streamflow losses at the catchment level was IAP density, followed by vegetation age, the shape of the streamflow reduction curves and the availability of additional water (Figure 6). Uncertainty in precipitation and the assignment of species to streamflow reduction curves did not contribute significantly to total uncertainty at the quaternary catchment level. .

4. Discussion

Invasive alien plants significantly reduce runoff in heavily invaded catchments in South Africa. The South African catchments experiments, initiated out of concern about the water-use impact of forestry species, are useful for understanding and predicting the impact of IAPs on water resources (Cullis et al., 2007; Le Maitre et al., 2019; Versfeld et al., 1998). Here we have reanalysed all the available data on streamflow reductions from the South African catchments experiments. Our analysis confirms previous work, showing that fast growing species, such as Eucalypts, reduce streamflow to a greater extent than slow growing species, and that the environmental conditions within each catchment have a large effect. But there remains considerable uncertainty in the streamflow reduction, particularly in young plantations. This uncertainty has been unaccounted for in previous studies building on the results of these experiments. Propagating this uncertainty to regional estimates of the impact of IAPs on streamflow produces results in broad agreement with previous studies, but with high uncertainty in many catchments. Differences of up to 23.2 million m³ per annum between upper and lower estimates of runoff loss are obtained within individual catchments. The relevance of the range in probable reduction estimates for decision makers can be emphasized by restating these numbers in terms of water security for the largest population center in the region, the City of Cape Town. Cape Town's 5 major dams are fed by sub-catchments of the Breede, Berg, and Olifants river systems. The upper and lower estimates of streamflow loss to IAPs in the quaternary catchments surrounding these dams are 20.3 and 43.4 million m³ per annum. Given the city's water use target of 0.45 million m³ per day at the height of the 'day-zero' drought, this volume of water translates into 45 and 97 days of water supply - a range of 52 days water supply.

Despite close agreement with the results of Le Maitre et al. (2016) for most catchments, in this study we estimate lower streamflow losses to IAPs for high-runoff catchments and overall. Given that we use the same data for IAP density, the same constraint on total annual catchment runoff and similar assignment of species to reduction curves, the remaining explanatory factors are pixel vegetation age, curve shape and additional water availability. Our estimates of vegetation age are higher than theirs (23 years vs 15 years), and hence are likely to produce higher estimates of streamflow reduction, not lower. Despite different methodologies for calculating the area in which additional water is available, our estimated total riparian area and groundwater availability is similar to theirs. However, for the range of vegetation ages common in mountain catchments of the CFR (10-30 years) the streamflow reduction curves

fitted here estimate lower mean runoff reductions than those of Scott & Smith (1997). In particular, lower reductions estimated for Pines under sub-optimal growing conditions - the IAP species most common in mountain catchments where the greatest runoff reductions occur (Kotze et al., 2010; Le Maitre et al., 2019) – are the most likely cause for our lower streamflow losses.

Partitioning and quantifying the sources of uncertainty in streamflow losses, as we have in this study, suggests paths for future research and refinement of existing estimates. While uncertainty in the assignment of species to curves did not influence total uncertainty greatly, the shape of the curves themselves did. High variability in the magnitude of streamflow reduction occurs for species assigned to the sub-optimal species curves. The influence of increasing water use within species with increasing evapotranspiration and interception is accounted for in both the age and growing condition covariates. A model that integrates these proxies into a single covariate could perhaps better account for the variation seen in the catchments experiments. The choice of covariate would, however, be limited to those that could be calculated from existing historical data e.g. basal area (Le Maitre & Versfeld, 1997).

Unsurprisingly uncertainty in IAP density was the most important contributor to overall uncertainty. This uncertainty is exacerbated by additional uncertainty unaccounted for here due to change in IAP density that has occurred since the mapping done by Kotze et al. (2010) was completed in 2007-2008 (van Wilgen et al., 2020). Without management intervention, IAPs can spread and increase cover up to 10% per year (van Wilgen & le Maitre, 2013; van Wilgen et al., 2020). Of particular concern is the assumption that IAP densities in riparian areas are the same as adjacent drylands. IAP densities in riparian zones often exceed those of adjacent drylands, and thus our assumption further biases our estimates of streamflow losses downwards. Kotze et al. (2010) do include a map of riparian invasion densities, but these have been reported as unreliable. Uncertainty in additional water availability is another major source of uncertainty in our model. This uncertainty, combined with unreliable IAP riparian density estimates, suggests that water loss to IAP in riparian zones is likely to be the largest source of uncertainty and error unaccounted for in our streamflow reduction estimates. When evaluated separately, as done here, the individual components of uncertainty do not sum to the total overall uncertainty due to interactions among components. This behavior suggests interaction among the components evaluated. While it is not possible to analytically evaluate these interactions using the model as posed here, collinearity among input parameters is the most likely explanation. For example, high uncertainty in multiple input variables can be expected in high rainfall, remote mountain

catchments.

The IAP density maps used here are intended for use at the tertiary catchment scale, but decisions regarding management interventions are made at much finer scales. Allocating limited resources to manage IAPs requires balancing costs and benefits that are influenced by fine scale variation in variables such as topography, accessibility, IAP density and runoff losses (Marais & Wannenburg, 2008; McConnachie et al., 2012). Ideally, densities for each pixel in this analysis would be available. New developments in satellite remote sensing and the availability of open data are facilitating the production of these maps at resolutions as fine as 10 m (Masemola et al., 2020). This analysis also underestimates the contribution of uncertainty in rainfall to total uncertainty because the uncertainty we report is summarized at the quaternary catchment scale. Rainfall is sampled independently for each pixel, with no reference to the rainfall values sampled in neighbouring pixels. There will, however, be strong spatial auto-correlation among neighbouring pixels. Hence when summing multiple pixels to estimate uncertainty at large scales, their importance will be underestimated. Indeed when we inspect the median absolute deviation of pixel-level streamflow reduction estimates rather than those calculated at the quaternary catchment level, the importance of rainfall becomes far greater (Figure S4).

Uncertainty in runoff predictions can be reduced by comparing predictions to observations from gauged catchments using a likelihood measure (Beven & Binley, 1992; Kavetski et al., 2006; Vrugt & Sadegh, 2013). Input parameter priors can be updated based on their likelihood given the observational data and predictions will be based on these updated parameter sets. While observations from gauged catchments were used to parameterize the effect of IAPs on water resources in this study, no observations are available against which the streamflow modelled here could be directly compared. However, the regionalization approach outlines a framework to constrain output uncertainty when data from gauged catchments is not available (Hughes et al., 2010; Kapangaziwiri et al., 2012; Wagener & Wheater, 2006). By comparing hydrological behaviour to those obtained in similar basins, calculated uncertainties can be reduced through the elimination of parameter sets that produce unrealistic scenarios. An adaptation of this approach may be possible for the estimation of IAP impacts. The model outlined here would be more amenable to this approach if streamflow reductions were estimated over multiple consecutive years, allowing the temporal co-evolution of modelled outputs such as runoff reduction, naturalized runoff, age and invasive density to be constrained. However, any approach that attempts to constrain the behaviour of hydrological models using only summary

statistics or aggregate behaviour without properly describing the full range of response observed in the data will lead to underestimating the variability of modelled behaviour. This issue further emphasizes the need to fully characterize and report on the uncertainty in fitted responses in paired catchment experiments, and propagate uncertainty to subsequent analyses.

The data from South African catchment experiments has been crucial for developing an understanding of the impacts of both afforestation and IAPs on water resources nationally. The full value of these data have yet to be realized and, as we show in this study, further analysis can improve the information available to decision makers. Analysing and propagating the uncertainty in these data provides more reliable estimates of IAP impacts on water resources, but requires the input data upon which models are built to be openly available. Simple models and summary statistics often do not suffice when attempting to fully describe the variability in drivers of hydrological processes. We hope this approach will be facilitated by ongoing efforts to preserve and extend the data from South African catchments experiments (e.g Slingsby et al, this issue), and future programmes to map the distribution of water resources and IAPs.

Acknowledgements

We are grateful to Adam Wilson for sharing climate and fire data. GM and JS were supported by the National Research Foundation of South Africa through (Grant No. 118593) as part of the *RReTool: Rapid and repeatable tools for monitoring and mitigating global change impacts on natural resources project*. The funders had no role in study design, data collection and analysis, decision to publish, or preparation of the manuscript.

Data availability

Code and data to reproduce our analyses are available at <https://github.com/GMoncrieff/streamflow-reduction>.

Bibliography

- Arachchige, C. N. P. G., Prendergast, L. A., & Staudte, R. G. (2020). Robust analogues to the Coefficient of Variation. *Journal of Applied Statistics*, 1-23.
- Bailey, A., & Pitman, W. V. (2015). Water Resources of South Africa, 2012 Study (WR2012). WRC, South Africa.
- Bennett, B. M., & Kruger, F. J. (2013). Ecology, forestry and the debate over exotic trees in South Africa. *Journal of Historical Geography*, 42, 100–109.
- Bergh, N. G., Verboom, G. A., Rouget, M., & Cowling, R. M. (2014). Vegetation types of the greater cape floristic region. *Fynbos: ecology, evolution, and conservation of a megadiverse region*, Oxford University Press, USA.
- Beven, K., & Binley, A. (1992). The future of distributed models: Model calibration and uncertainty prediction. *Hydrological Processes*, 6(3), 279–298.
- Bischoff-Mattson, Z., Maree, G., Vogel, C., Lynch, A., Olivier, D., & Terblanche, D. (2020). Shape of a water crisis: practitioner perspectives on urban water scarcity and ‘Day Zero’ in South Africa. *Water Policy*, 22(2), 193–210.
- Bosch, J. M., & Hewlett, J. D. (1982). A review of catchment experiments to determine the effect of vegetation changes on water yield and evapotranspiration. *Journal of Hydrology*, 55(1), 3–23.
- Brown, A. E., Zhang, L., McMahon, T. A., Western, A. W., & Vertessy, R. A. (2005). A review of paired catchment studies for determining changes in water yield resulting from alterations in vegetation. *Journal of Hydrology*, 310(1-4), 28-61
- Calder, I. R. (1985). What are the limits on forest evaporation?—Comment. *Journal of Hydrology*, 82(1-2), 179–184.
- Calder, I. R. (2005). *Blue revolution: Integrated land and water resource management*. Routledge, UK.
- Carpenter, B., Gelman, A., Hoffman, M. D., Lee, D., Goodrich, B., Betancourt, M., Brubaker, M., Guo, J., Li, P., & Riddell, A. (2017). Stan: A probabilistic programming language. *Journal of Statistical Software*, 76(1).
- Clulow, A. D., Everson, C. S., & Gush, M. B. (2011). The long-term impact of Acacia mearnsii trees on evaporation, streamflow and ground water resources. *Water Research Commission Report No. TT505/11*, WRC, South Africa.

- Cullis, J. D. S., Görgens, A. H. M., & Marais, C. (2007). A strategic study of the impact of invasive alien plants in the high rainfall catchments and riparian zones of South Africa on total surface water yield. *Water SA*, 33(1).
- Ferrari, S., & Cribari-Neto, F. (2004). Beta Regression for Modelling Rates and Proportions. *Journal of Applied Statistics*, 31(7), 799–815.
- Fick, S. E., & Hijmans, R. J. (2017). WorldClim 2: new 1-km spatial resolution climate surfaces for global land areas. *International journal of climatology*, 37(12), 4302–4315.
- Finley, A. O., Banerjee, S., & Carlin, B. P. (2007). spBayes: an R package for univariate and multivariate hierarchical point-referenced spatial models. *Journal of Statistical Software*, 19(4), 1.
- Gush, M. B., Scott, D. F., Jewitt, G. P. W., Schulze, R. E., Lumsden, T. G., Hallows, L. A., & Görgens, A. H. M. (2002). Estimation of streamflow reductions resulting from commercial afforestation in South Africa. *Water Research Commission Report No. TT173/02*, WRC, South Africa.
- Harmon, M. E., Fasth, B., Halpern, C. B., & Lutz, J. A. (2015). Uncertainty analysis: an evaluation metric for synthesis science. *Ecosphere*, 6(4), art63.
- Hofste, R. W., Kuzma, S., Walker, S., Sutanudjaja, E. H., Bierkens, M. F. P., Kuijper, M. J. M., Sanchez, M. F., Beek, R. V., Wada, Y., Rodríguez, S. G., & Reig, P. (2019). Aqueduct 3.0: Updated Decision-Relevant Global Water Risk Indicators.
- Hughes, D. A., Kapangaziwiri, E., & Sawunyama, T. (2010). Hydrological model uncertainty assessment in southern Africa. *Journal of Hydrology*, 387(3), 221–232.
- Jensen, J. L. W. V. (1906). Sur les fonctions convexes et les inégalités entre les valeurs moyennes. *Acta Mathematica*. 30 (1): 175–193.
- Kalognomou, E.-A., Lennard, C., Shongwe, M., Pinto, I., Favre, A., Kent, M., Hewitson, B., Dosio, A., Nikulin, G., & Panitz, H.-J. (2013). A diagnostic evaluation of precipitation in CORDEX models over southern Africa. *Journal of Climate*, 26(23), 9477–9506.
- Kapangaziwiri, E., Hughes, D. A., & Wagener, T. (2012). Incorporating uncertainty in hydrological predictions for gauged and ungauged basins in southern Africa. *Hydrological Sciences Journal*, 57(5), 1000–1019.
- Kavetski, D., Kuczera, G., & Franks, S. W. (2006). Bayesian analysis of input uncertainty in hydrological modeling: 2. Application. *Water Resources Research*, 42(3).
- Kotze, I., Beukes, H., van der Berg, E., & Newby, T. (2010). National Invasive Alien Plant Survey. Tech. Rep. Report No. GW/A/2010/21. ARC-Institute for Soil, Climate and Water (ARC-

ISCW), South Africa.

Kraaij, T., Baard, J. A., Arndt, J., Vhengani, L., & van Wilgen, B. W. (2018). An assessment of climate, weather, and fuel factors influencing a large, destructive wildfire in the Knysna region, South Africa. *Fire Ecology*, 14(2), 4.

Le Maitre, D., Görgens, A., Howard, G., & Walker, N. (2019). Impacts of alien plant invasions on water resources and yields from the Western Cape Water Supply System (WCWSS). *Water SA*, 45(4), 568–579.

Le Maitre, D. C., Blignaut, J. N., Clulow, A., Dzikiti, S., Everson, C. S., Görgens, A. H. M., & Gush, M. B. (2020). Impacts of Plant Invasions on Terrestrial Water Flows in South Africa. In B. W. van Wilgen, J. Measey, D. M. Richardson, J. R. Wilson, & T. A. Zengeya (Eds.) *Biological Invasions in South Africa*. Springer.

Le Maitre, D. C., Forsyth, G. G., Dzikiti, S., & Gush, M. B. (2016). Estimates of the impacts of invasive alien plants on water flows in South Africa. *Water SA*, 42(4), 659–672.

Le Maitre, D. C., Gush, M. B., & Dzikiti, S. (2015). Impacts of invading alien plant species on water flows at stand and catchment scales. *AoB Plants*, 7.

Le Maitre, D. C., & Versfeld, D. B. (1997). Forest evaporation models: relationships between stand growth and evaporation. *Journal of Hydrology*, 193(1), 240–257.

LeBauer, D. S., Wang, D., Richter, K. T., Davidson, C. C., & Dietze, M. C. (2013). Facilitating feedbacks between field measurements and ecosystem models. *Ecological Monographs*, 83(2), 133–154.

LTSS (2002). Land types of South Africa: Digital map (1:250 00 scale) and soil inventory databases. ARC-Institute for Soil, Climate and Water (ARC-ISCW), South Africa.

Marais, C., & Wannenburg, A. (2008). Restoration of water resources (natural capital) through the clearing of invasive alien plants from riparian areas in south africa — costs and water benefits. *South African Journal of Botany*, 74(3), 526 – 537

Masemola, C., Cho, M. A., & Ramoelo, A. (2020). Towards a semi-automated mapping of australia native invasive alien acacia trees using sentinel-2 and radiative transfer models in south africa. *ISPRS Journal of Photogrammetry and Remote Sensing*, 166, 153 – 168.

McConnachie, M. M., Cowling, R. M., van Wilgen, B. W., & McConnachie, D. A. (2012). Evaluating the cost-effectiveness of invasive alien plant clearing: A case study from south africa. *Biological Conservation*, 155, 128 – 135.

Midgley, D. C., Pitman, W. V., & Middleton, B. J. (1994). The surface water resources of South Africa 1990 (WR90). Tech. rep., Water Research Commission, Pretoria. Mucina, L., &

Rutherford, M. C. (Eds.) (2006). *The vegetation of South Africa, Lesotho and Swaziland*.

Strelitzia 19. South African National Biodiversity Institute, South Africa.

Nel, J. L., Le Maitre, D. C., Roux, D. J., Colvin, C., Smith, J. S., Smith-Adao, L. B., Maherry, A., & Sitas, N. (2017). Strategic water source areas for urban water security: Making the connection between protecting ecosystems and benefiting from their services. *Ecosystem Services*, 28, 251–259.

Otto, F.E., Wolski, P., Lehner, F., Tebaldi, C., Van Oldenborgh, G.J., Hogesteegeer, S., Singh, R., Holden, P., Fučkar, N.S., Odoulami, R.C. & New, M., (2018). Anthropogenic influence on the drivers of the Western Cape drought 2015–2017. *Environmental Research Letters*, 13(12), p.124010.

Pienaar, L., & Boonzaaier, J. (2018). Drought policy brief Western Cape Agriculture. Western Cape Department of Agriculture (WCDoA) and the Bureau for Food and Agricultural Policy (BFAP), South Africa.

Qiao, L., Zou, C. B., Will, R. E., & Stebler, E. (2015). Calibration of SWAT model for woody plant encroachment using paired experimental watershed data. *Journal of Hydrology*, 523, 231–239. R Core Team (2017). *R: A Language and Environment for Statistical Computing*. Vienna, Austria: R Foundation for Statistical Computing.

Reichert, P., & Borsuk, M. E. (2005). Does high forecast uncertainty preclude effective decision support? *Environmental Modelling & Software*, 20(8), 991–1001.

Schreiner, B. G., Mungatana, E. D., & Baleta, H. (2018). Impacts of Drought Induced Water Shortages in South Africa: Economic Analysis. *Water Research Commission Report No. 2604/1*, WRC, South Africa.

Schulze, R. E. (1997). *South African Atlas of Agrohydrology and Climatology: Contribution Towards a Final Report to the Water Research Commission on Project 492: Modelling Impacts of the Agricultural Environment on Water Resources*. *Water Research Commission Report No. TT82/96*, WRC, South Africa.

Scott, D. F., Le Maitre, D. C., & Fairbanks, D. H. K. (1998). Forestry and streamflow reductions in South Africa: A reference system for assessing extent and distribution. *Water SA*, 24(3), 187–199.

Scott, D. F., Prinsloo, F.W. & Moses, G. (2000). *A re-analysis of the South African catchment afforestation experimental data*. *Water Research Commission Report No. TT810/1/00*, WRC, South Africa.

Scott, D. F., & Smith, R. E. (1997). Preliminary empirical models to predict reductions in total

and low flows resulting from afforestation. *Water SA*, 23(2), 135-140.

Slingsby, J. A., Merow, C., Aiello-Lammens, M., Allsopp, N., Hall, S., Mollmann, H. K., Turner, R., Wilson, A. M., & Silander, J. A. (2017). Intensifying postfire weather and biological invasion drive species loss in a Mediterranean-type biodiversity hotspot. *Proceedings of the National Academy of Sciences*, 114(18), 4697–4702.

Sousa, P. M., Blamey, R. C., Reason, C. J., Ramos, A. M., & Trigo, R. M. (2018). The 'Day Zero' Cape Town drought and the poleward migration of moisture corridors. *Environmental Research Letters*, 13(12), 124025.

Steynor, A. C., Hewitson, B. C., & Tadross, M. A. (2009). Projected future runoff of the Breede River under climate change. *Water SA*, 35(4).

van Deventer, H., van Niekerk, L., Adams, J., Dinala, M. K., Gangat, R., Lamberth, S. J., Lötter, M., Mbona, N., MacKay, F., Nel, J. L., Ramjukadh, C.-L., Skowno, A., & Weerts, S. P. (2020). National wetland map 5: An improved spatial extent and representation of inland aquatic and estuarine ecosystems in South Africa. *Water SA*, 46

van Wilgen, B. W., & le Maitre, D. C. (2013). Rates of spread in invasive alien plants in South Africa. Tech. rep., Council for Scientific and Industrial Research, Stellenbosch.

van Wilgen, B. W., Le Maitre, D. C., & Cowling, R. M. (1998). Ecosystem services, efficiency, sustainability and equity: South Africa's Working for Water programme. *Trends in Ecology & Evolution*, 13(9), 378.

van Wilgen, B. W., Wilson, J. R., Wannenburg, A., & Foxcroft, L. C. (2020). The extent and effectiveness of alien plant control projects in South Africa. In B. W. van Wilgen, J. Measey, D. M. Richardson, J. R. Wilson, & T. A. Zengeya (Eds.) *Biological Invasions in South Africa*. Springer.

Vehtari, A., Gelman, A., & Gabry, J. (2017). Practical Bayesian model evaluation using leave-one-out cross-validation and WAIC. *Statistics and Computing*, 27(5), 1413–1432.

Versfeld, D. B., Le Maitre, D. C., & Chapman, R. A. (1998). *Alien invading plants and water resources in South Africa: a preliminary assessment*. Water Research Commission Report No. TT99/98, WRC, South Africa.

Vrugt, J. A., & Sadegh, M. (2013). Toward diagnostic model calibration and evaluation: Approximate Bayesian computation. *Water Resources Research*, 49(7), 4335–4345.

Wagener, T., & Wheeler, H. S. (2006). Parameter estimation and regionalization for continuous rainfall-runoff models including uncertainty. *Journal of Hydrology*, 320(1), 132–154.

Wilson, A. M., Latimer, A. M., Silander Jr, J. A., Gelfand, A. E., & De Klerk, H. (2010). A

hierarchical Bayesian model of wildfire in a Mediterranean biodiversity hotspot: implications of weather variability and global circulation. *Ecological Modelling*, 221(1), 106–112.

Wilson, A. M., & Silander Jr, J. A. (2014). Estimating uncertainty in daily weather interpolations: a Bayesian framework for developing climate surfaces. *International Journal of Climatology*, 34(8), 2573–2584.

Yanai, R. D., See, C. R., & Campbell, J. L. (2018). Current Practices in Reporting Uncertainty in Ecosystem Ecology. *Ecosystems*, 21(5), 971–981.

Zhang, L., Dawes, W. R., & Walker, G. R. (2001). Response of mean annual evapotranspiration to vegetation changes at catchment scale. *Water Resources Research*, 37(3), 701–708.

Table and Figures

| Name | LOOIC |
|---|--------------|
| Age + Condition + Species + Age/Condition | -508.90 |
| Age + Condition + Species + Age/Condition + Age/Species | -506.45 |
| Age + Condition + Species + Age/Species | -445.10 |
| Age + Condition + Species | -418.16 |

Table 1. Comparison of beta regression models fitted to the South African catchment data from (Scott et al., 2000). Models appear in order of performance measured using the leave-one-out cross-validation (LOO) information criterion. Lower LOOIC values indicate better performance.

Fig 1. Overview of the process used to model runoff reductions by invasive alien plants. Parameters were sampled at three scales during each model iteration. At the highest level parameters were sampled once for each iteration and shared across all catchments. At the next level, parameters were sampled separately in each catchment. At the lowest level, parameters were sampled independently for each pixel. Mean annual runoff was calculated at the pixel level and then summed to provide a catchment-level estimate for each iteration. Colour coding indicates where each component and its related parameters were incorporated into the final calculation of pixel-level runoff reduction. Each colour corresponds to a subsection within the methods description.

Fig. 2. Streamflow reduction curves to the South African catchment data using the best fitting beta regression model. Dots indicate data points for each year. Solid lines indicate mean predictions, while light shaded areas indicate 95% predictive intervals and dark shading indicates 50% intervals. Dotted and Dashed lines indicate the curves fitted by Scott & Smith (1997) for optimal and suboptimal growing conditions respectively.

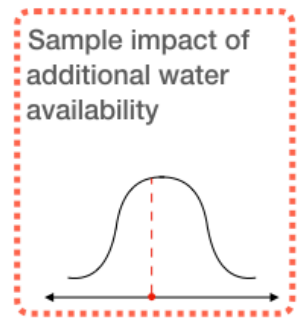
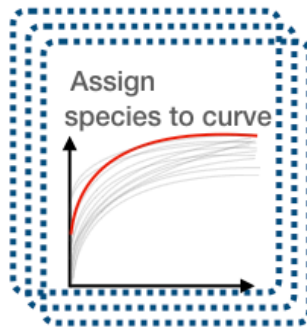
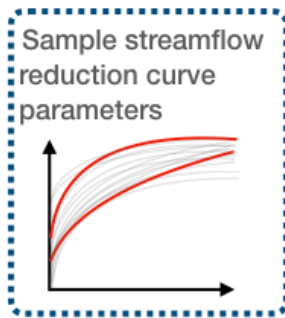
Fig. 3. Comparison of estimated streamflow reductions for quaternary catchments with results from Le Maitre et al. (2016). Vertical bars show 95% quantile intervals for predicted streamflow reductions. The solid line shows the 1:1 relationship and the dashed line the linear fit

Fig. 4. Streamflow losses to invasive alien plants estimated within 306 quaternary catchments of the Greater Cape Floristic Region. Upper and lower bounds show 95% quantile interval estimates. Reductions are shown as percentages of predicted naturalized runoff.

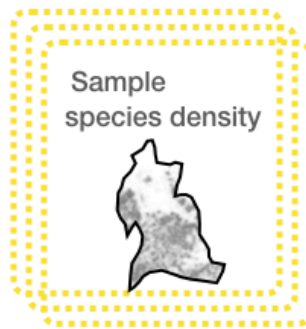
Fig. 5. Uncertainty in estimates of streamflow losses to invasive alien plants within quaternary catchments of the Greater Cape Floristic Region represented as the robust coefficient of variation (RCV_M), and the median absolute deviation (MAD).

Fig. 6. Total uncertainty in streamflow reduction, calculated as the sum of median absolute deviation for all quaternary catchments, attributed to uncertainty in: the density of invasive alien plants, vegetation age, the shape of the streamflow reduction curve, the availability of additional water from groundwater or riparian sources, mean annual rainfall, and the assignment of species to streamflow reduction curves. Each source of uncertainty is represented as a percent of the total uncertainty when all sources are included.

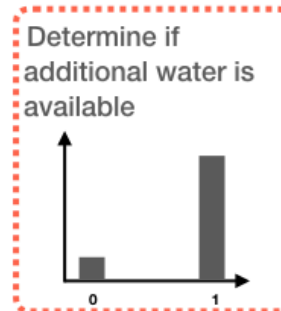
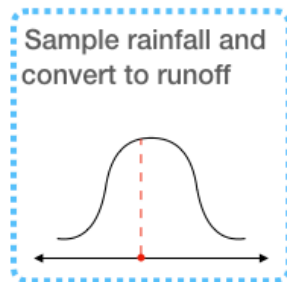
For each model run:



For each catchment:



For each pixel:



Calculate:

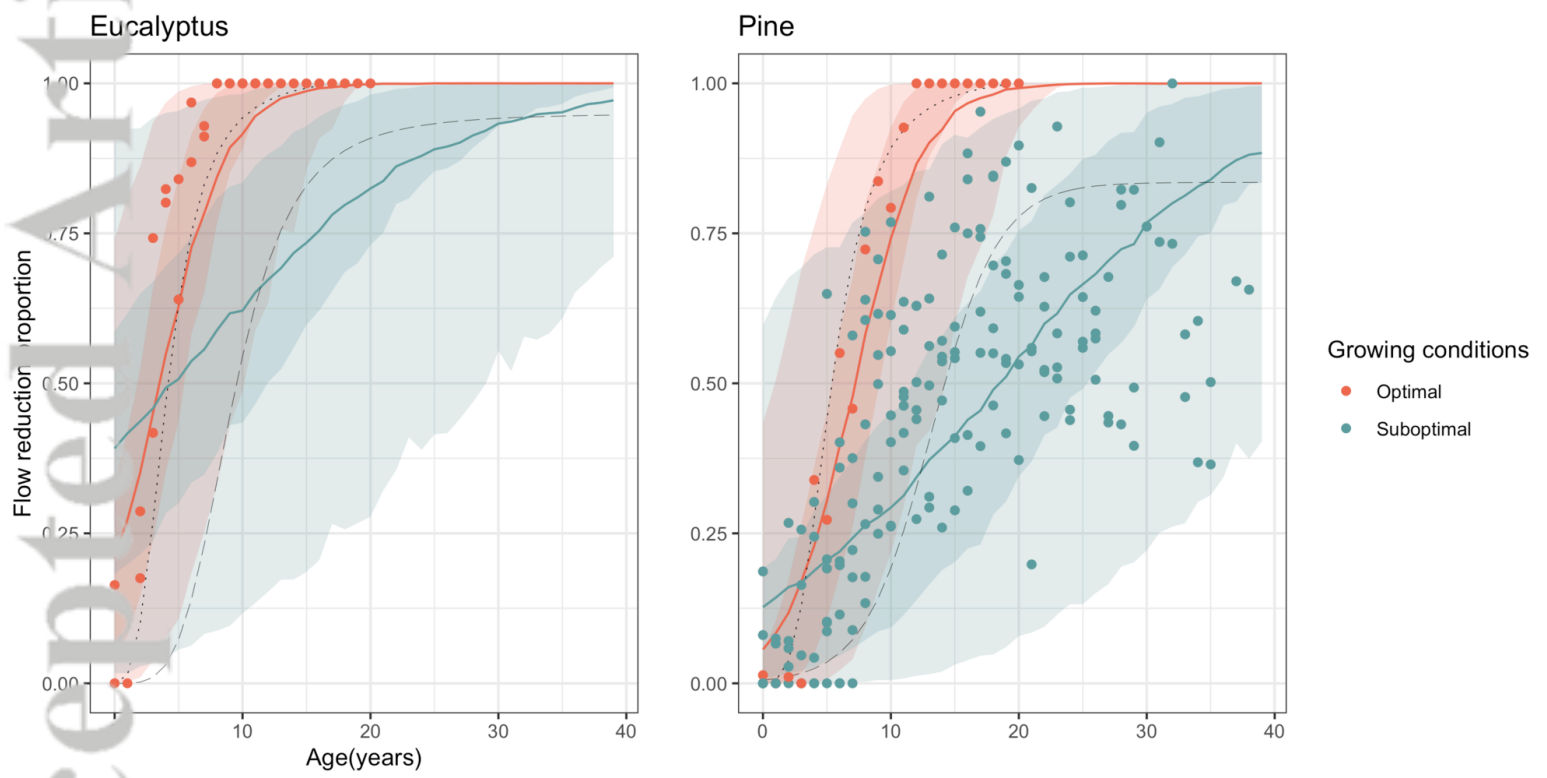
For species j in pixel i

$$1. \text{Reduction}_{ij} = f(\text{age}_i) \cdot \text{density}_j$$

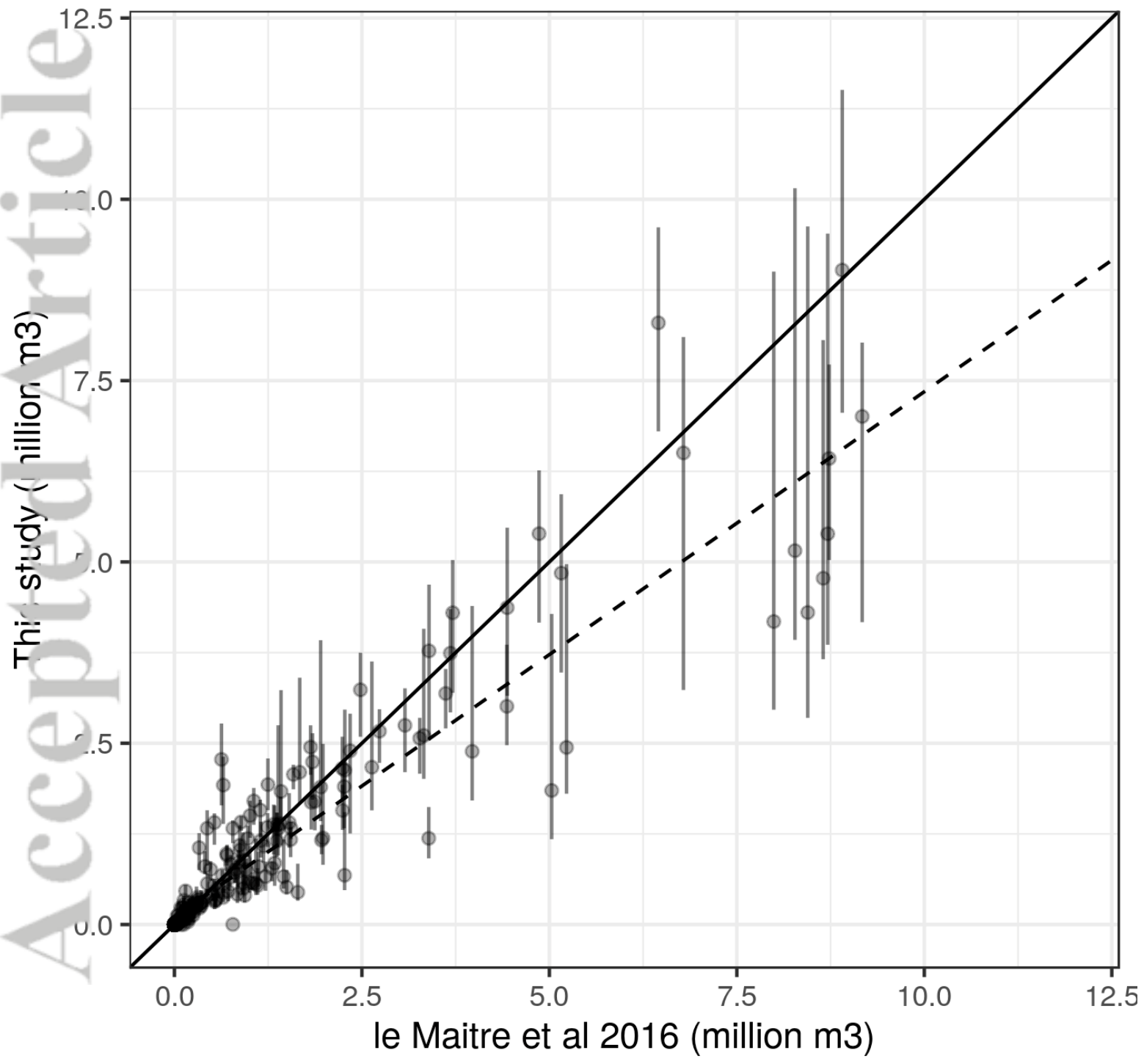
Where $f()$ is the reduction curve applicable for species j

$$2. \text{PotentialRunoff}_i = \text{Runoff}_i \cdot \text{AdditionalWater}_i$$

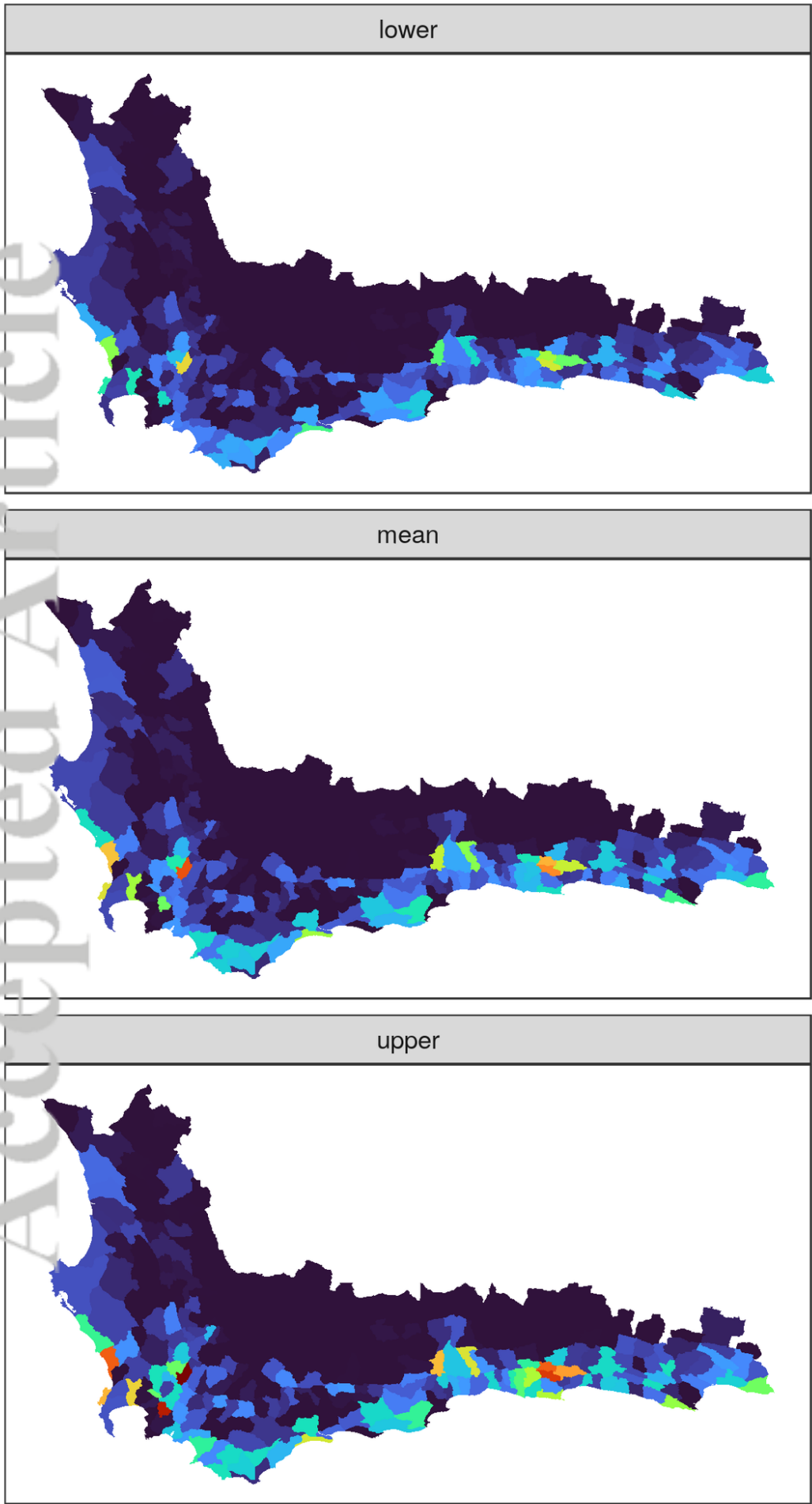
$$3. \text{RunoffReduction}_i = \text{PotentialRunoff}_i \cdot \sum_j \text{Reduction}_{ij}$$



HYP_14161_figure2.png

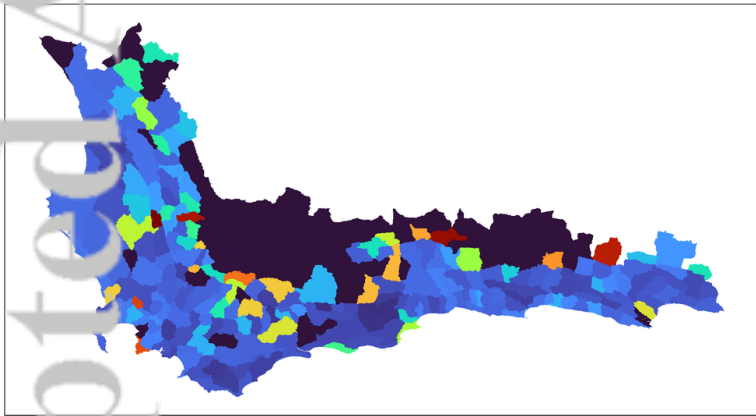


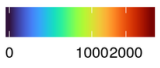
HYP_14161_figure3.png

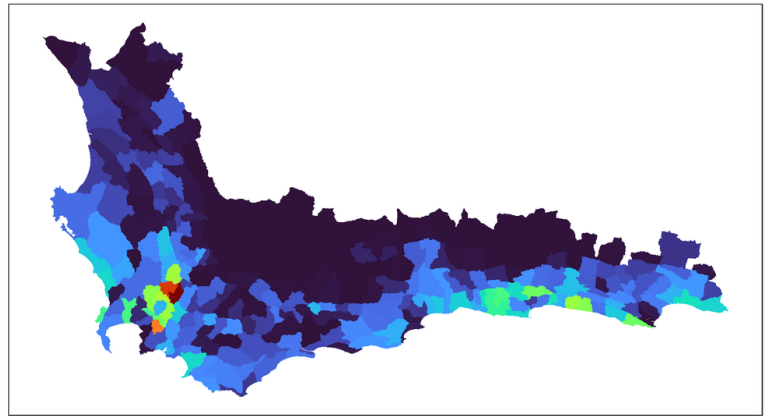


HYP_14161_figure4.png

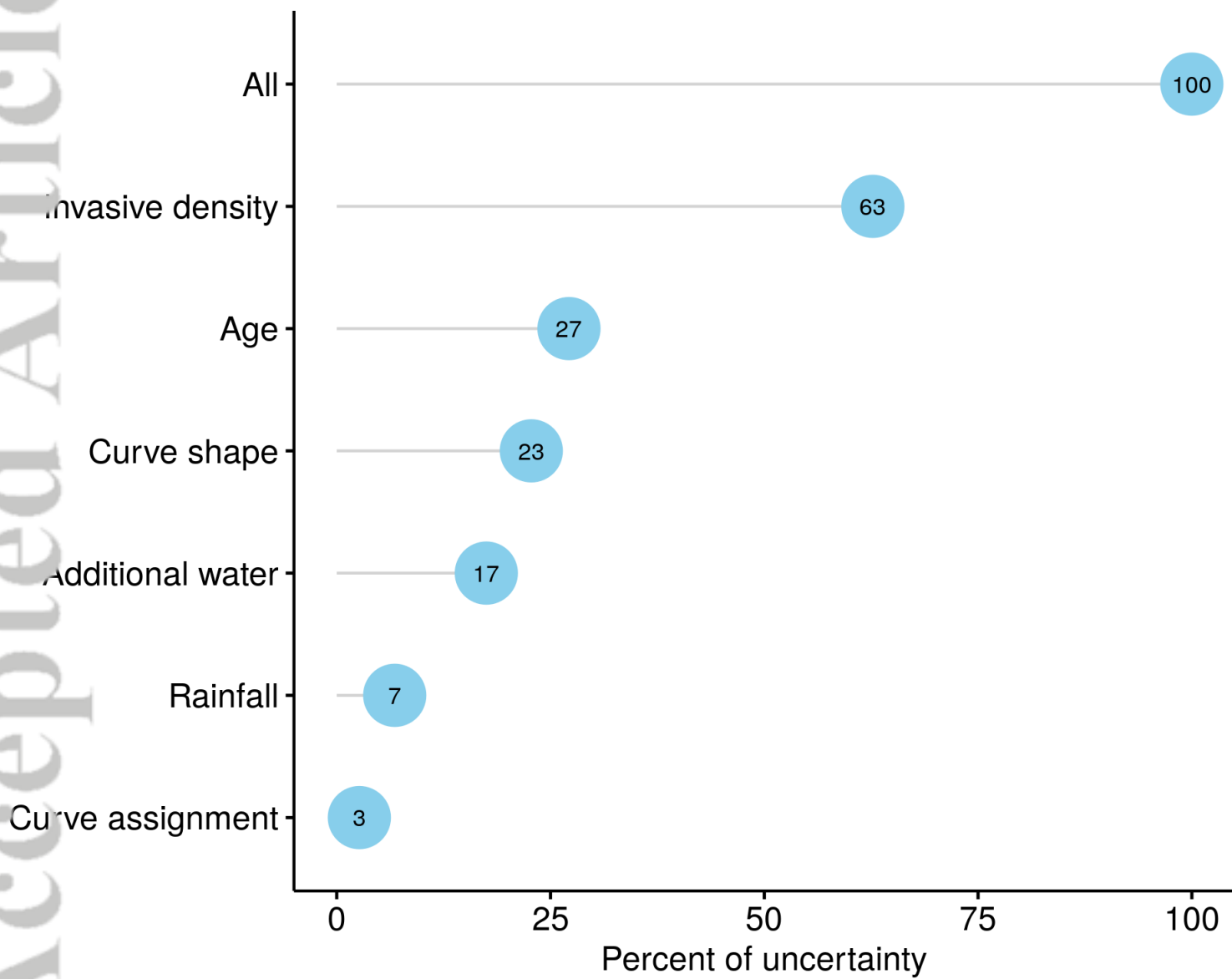
Coefficient of variation  0.0 0.2 0.4 0.6 0.8



Median absolute deviation (M)  0 10002000



HYP_14161_figure5.png



HYP_14161_figure6.png